Int. J. Heat Mass Transfer. Vol. 36, No. 6, pp. 1639–1647, 1993
Printed in Great Britain

0017 9310/93 $6.00+0.00
Pergamon Press Ltd

Heat transfer due to a round jet impinging normal to a flat surface

A. K. MOHANTY and A. A. TAWFEK†
Department of Mechanical Engineering, Indian Institute of Technology, Kharagpur, India

(*Received* 28 *November* 1991 *and in final form* 22 *April* 1992)

Abstract—Heat transfer measurements from an isothermal plate due to an impinging air-jet from 3, 5 and 7 mm diameter circular nozzles were carried out for nozzle to plate distance ratio varied from 4 to 58, and the nozzle Reynolds number from 4860 to 34 500. Local heat transfer rates have been estimated from the outputs of three-wire differential thermocouple heat flux sensors. From the highest value at the impingement point, the heat transfer rate decays exponentially with radial distance. The effective area for a nozzle has been defined when a non-dimensional heat transfer rate, H, has decreased from unity to e^{-1}. $\bar{H} = 0.54$ is a good average value.

1. INTRODUCTION

JET IMPINGEMENT yields higher heat transfer rates than are possible by most other methods of single phase forced convection. In a survey article, Martin [1] enumerated its utility in annealing of metal and plastic sheets, tempering of glass, drying of textiles, veneer, paper and film material, curing processes and in the protection of surfaces exposed to high local heat fluxes. The wide spectrum of applications has called for the use of different shapes and sizes of nozzles, nozzle to surface distance, angle of impingement and coolant fluids.

In one of the earliest studies, Perry [2] measured overall heat transfer coefficients from a hot gas jet to a plane surface for jet to plate spacings greater than eight jet diameters, and observed a two-fold increase in heat transfer compared to parallel flow at the same jet velocity. Vickers [3] reported results for low jet Reynolds number to a maximum of 950. Gardon *et al.* [4, 5] noted that the impingement point heat transfer in the turbulent regime is maximum when the nozzle is 6–7 diameters away from the plate. Huang [6] derived empirical correlations for local as well as average heat transfer rates of a single jet dependent solely on Reynolds number. Vallis *et al.* [7] used the electrolytic mass transfer technique to study the radial distribution of convective heat transfer coefficients from the stagnation point to the fully developed wall jet region, for a range of Reynolds number between 3.8×10^3 to 23×10^3 and for nozzle to plate distances 5 to 50 diameters. Sparrow and Lovell [8] used the naphthalene mass transfer technique to investigate the effects of the angle of inclination of the jet relative to the surface from 30° to 90°. Obot *et al.* [9] reported studies to determine the effects of nozzle inlet shape, e.g. contoured and sharp-edged, and nozzle length to diameter ratio on impingement heat transfer. Wang *et al.* [10, 11] have reported numerical results for a circular impinging jet on a solid surface with non-uniform temperature and wall heat flux. Literature on slot jets or liquid cooling are yet another extensive set, and are kept outside the present study. Reference may be made to a recent study by Vadet *et al.* [12], for instance, for information on slot jets and water cooling.

The large number of investigations notwithstanding, uncertainties exist in two major aspects of impingement heat transfer. One is the transport rate value at the stagnation or impingement point, and the other on the effective area of cooling, or heating, by a jet. Measurements by strip or ring heaters, calorimetry and condensation [13], or analogy [7] methods are not very convenient for estimating heat transfer rates over small dimensions, such as the stagnation point. Gardon's [4, 5] heat flux sensor was a convenient device for local measurements. However, Gardon and coworkers observed [5] that the sensitivity of their sensors were at times 65% off, apparently due to conduction leakage.

Discrepancies in the stagnation point value are treated to be of minor importance [1], because practical interests often hinge on integral average transfer coefficients. But then one needs to know the effective area of influence of an impinging jet for the purpose of averaging. The practice in the literature in this respect is some what arbitrary. Sparrow and Lovell [8] present their average heat transfer values over 4 and 8 nozzle diameters, whereas Huang [6] used $12d$. More frequently, the area of the target plate is considered for the estimation of the average. For instance, Hrycak [13] used four nozzles of 3.18 to 12.7 mm diameter, z/d ratio from 2 to 20, impinging on a plate of $D = 152.4$ mm diameter. The average value for all cases was calculated on the basis of D. Such averages do not distinguish the effective radius of influence which must be varying for each of the configurations.

† Ship Engineering Department, Faculty of Engineering and Technology, Port-Said, Egypt.

NOMENCLATURE

a	sound speed [m s^{-1}]
Bi	Biot number, $R^2/k_f t$
d	nozzle diameter [m]
h	local heat transfer coefficient at any radius r [W m^{-2} K^{-1}]
h_0	impingement point heat transfer coefficient [W m^{-2} K^{-1}]
h_f	heat transfer coefficient at the edge of the effective area [W m^{-2} K^{-1}]
H	local heat transfer function, $(h-h_f)/(h_0-h_f)$
H_0	maximum value of the heat transfer function, $H_0 = 1$
$\bar{H}$	average value of the heat transfer function
k_f	thermal conductivity of the foil material [W m^{-1} K^{-1}]
M	Mach number
Nu	local Nusselt number at any radius r, based on nozzle diameter, hd/k
Nu_0	Nusselt number at the impingement point $h_0 d/k$
P_∞	static pressure [N m^{-2}]
P_0	stagnation pressure [N m^{-2}]
r	radial distance along the heat transfer surface [m]
r_{eff}	effective radius [m]
R	radius of the foil [m]
Re	Reynolds number, based on nozzle diameter, Vd/ν
t	thickness of the foil [m]
T	air temperature at the nozzle exit [K]
V	average nozzle velocity [m s^{-1}]
z	separation distance between nozzle and impingement surface [m].

The objectives of the present experiments are to overcome the above short comings. Gardon type heat flux sensors of 2 mm foil size permitting similar spatial resolutions have been used for local measurements. The sensor design and calibration have been improved and leakage restricted to 1% [14]. Results for the stagnation point and radial variation of heat transfer rates are obtained with improved accuracy. A method to uniquely determine the effective heat transfer area for a jet impinging on a surface has been suggested. For the same jet-target configuration and flow rate, the effective area can vary depending on the desired degree of cooling. For example, the effective area for an impingement drying process can be large compared to cooling in metallurgical processes or in electronic devices. The jet spacings would correspondingly differ. Such variations can be accomodated by the method we are suggesting.

2. EXPERIMENTAL SET-UP

The major components of the experimental set-up are: a blower and nozzle arrangement for creating the air-flow; a brass plate with variable heating arrangement and insulations; flow measuring devices and three-wire differential thermocouple heat flux sensors [14] for direct measurement of local heat transfer coefficients.

2.1. *Flow*

Air at moderate pressure from the blower with a by-pass arrangement, Fig. 1, is led to the nozzle through a gateway-valve for flow control. Three nozzles of outlet diameters 3, 5 and 7 mm were used, one at a time, for creating the jet flow. The nozzles were machined from brass rods 37 mm OD. The diameter of the nozzle hole at inlet was 25 mm, tapering to the respective exit value. The inlet to outlet area ratios for the nozzles were, thus, 70, 25 and 12.8, and the corresponding velocity head ratios 4900, 625 and 163. These values suggested that the velocity heat at the nozzle inlet is negligible compared to the outlet, and the static pressure measured at the inlet is, practically, the total pressure, P_0, for the nozzle flow. The inlet static pressure measurement was utilized for the estimation of the air flow rate at the nozzle exit. An orifice plate located on the blower delivery pipe was used as a cross-check.

2.2. *Nozzle and heated plate*

The nozzle was screwed on to a holding-plate with a hole, and the assembly held vertical on an angle-iron frame as shown in Fig. 1. The verticality of the nozzle was monitored by a protractor attached to the assembly, as well as by a plumb-line. A scale was fitted to the frame for measuring the distance between the nozzle exit and the hot plate meant for impingement. The nozzle inlet was connected to the blower discharge through a thick, flexible acrylic pipe.

The heated horizontal plate was 180 mm diameter, 6 mm thick and made of brass. The plate was mounted flush on a cylindrical asbestos base which also housed the heating elements; one surrounding the other. The inner one served as the main heater and other as the guard heater; power supply to each controlled separately, see Fig. 1. The closed-bottom asbestos cylinder had a minimum wall thickness of 15 mm and a 30 mm base-plate with grooves for accommodating the heating elements. When flush-fitted, the distance between the heater coils and the plate underside was

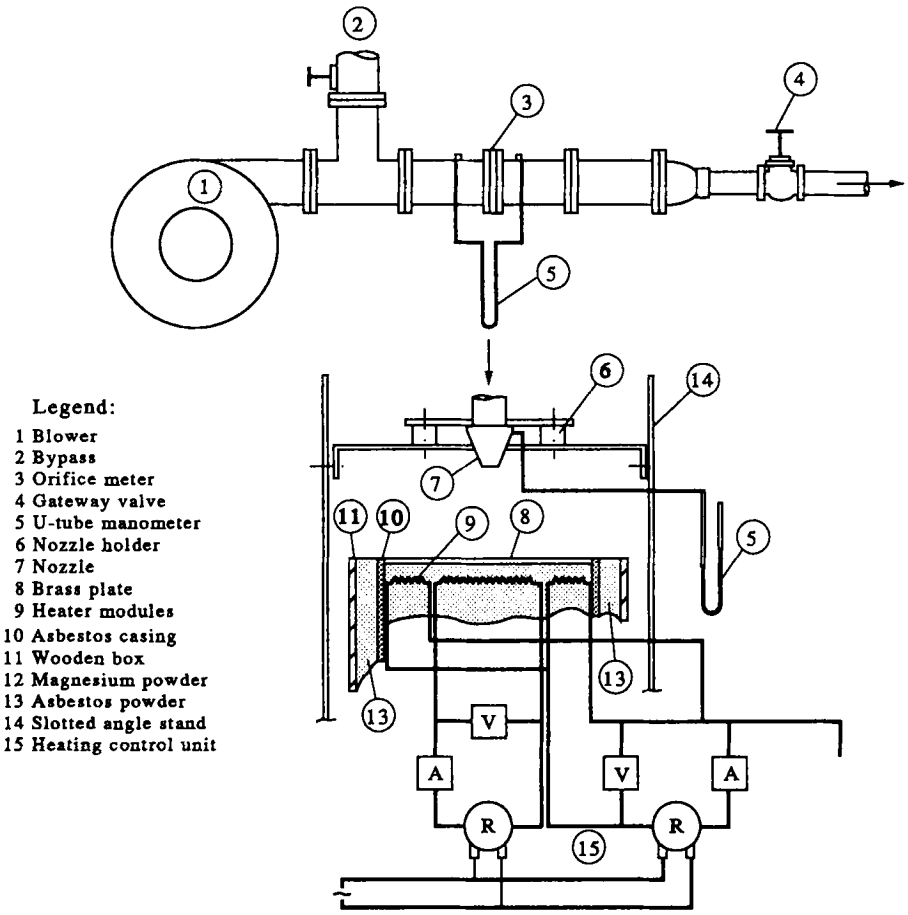

FIG. 1. Schematic view of experimental set-up.

approximately 30 mm. This space was filled with magnesium oxide powder to eliminate free-convection cells, and the heat from the coils was conducted through the powder to the plate. Lead wires to the heating elements were connected through two holes on the base plate. The entire assembly was placed in a rectangular wooden box 450 mm × 300 mm and 250 mm deep. The space between the assembly and the box wall was filled with asbestos powder. When placed under the nozzle for jet impingement, the horizontality of the plate was ensured by spirit-level measurements.

2.3. *Heat flux sensor*

The theory, design, fabrication and calibration of 3-wire heat flux sensors have been elaborated in ref. [14], and application demonstrated in ref. [15]. Each sensor is made of a copper tubing as a base, covered by a thin constantan foil at one end. When the assembly (sensor) is placed flush in a heated body, the heat loss from the foil surface causes a temperature differential across the foil centre to its periphery on the copper tube. The rate of heat loss, which is also the hot body local heat flux, is then measured though the differential temperature across the foil radius.

The sensors used in the present experiments, 17 in number, were made of 3 mm OD copper tube, 0.23 mm thick constantan foil of effective diameter 2 mm. Thirty two gage copper and constantan wires were used for thermometry readings.

The sensors, first calibrated on a spherical heating apparatus [14], were mounted on the test plate along the x and y axes on either side of the plate centre, see Fig. 2. The hole diameter on the plate was nominally 3 mm and a pre-calibrated sensor was first shrunk by cold treatment and then fitted snugly onto the plate. Care was taken to avoid polishing the sensor foil after calibration, for, otherwise, the sensor sensitivity could change due to reduction in the foil thickness [14].

It will be noted from Fig. 2 that the locations of the sensors were placed equally to the left and right of the plate centre so that a cross-check for the readings of the local values of h could be made under perpendicular impingement condition. The sensors were placed closer (12.5 mm interval) to the plate centre, widening to 20 mm near the periphery. Out of the total 17 sensors, six were used along the y-axis covering 20 to 35 mm intervals. The sensor (thermocouple) wires, with teflon sleeves, were taken out through a hole in the wall of the asbestos heater module.

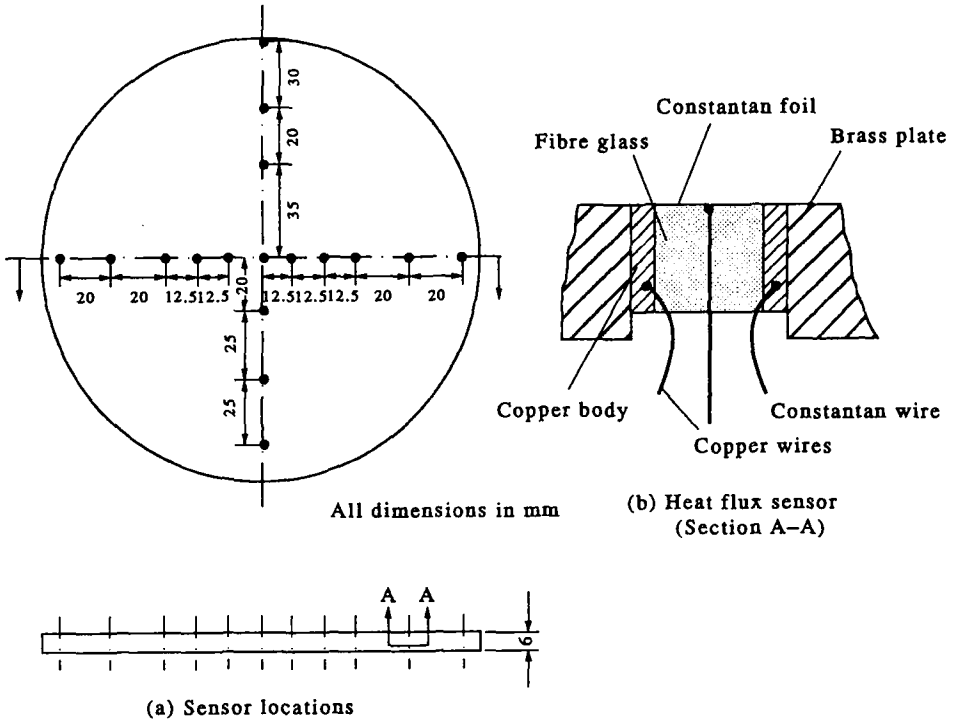

FIG. 2. Layout of heat flux sensors on plate surface.

3. TEST PROCEDURE

The variable parameters of experiments with each of the three nozzles were the nozzle flow rate, plate to nozzle distance, and the plate surface temperature.

3.1. *Velocity*

The nozzle length being short, typically 30 mm, and rapidly converging, the air flow through it could be considered isentropic for which the stagnation pressure is the value measured at the nozzle inlet of 25 mm diameter. Since the discharge is atmospheric, pressure P_∞, the isentropic relation gives

$$\frac{P_0}{P_\infty} = \left(1 + \frac{k-1}{2} M^2\right)^{k/k-1} \quad (1)$$

M being the Mach number and $k = 1.4$.

Equation (1) yields the flow Mach number when the measured value of P_0 is used. The maximum value of M, covered by the present experiments was 0.237.

The temperature of air measured by a thermometer at the nozzle exit is its stagnation value, and the static temperature is evaluated by using the value of M. The nozzle exit velocity is then obtained as $V = M \cdot a$, where $a = \sqrt{kRT}$ is the local speed of sound. The range of variations of the jet velocity at nozzle exit was 20–85 m s^{-1}, and the nozzle distance to diameter ratio (z/d) 4.3–58.

3.2. *Heat transfer*

The temperature of the air at the nozzle exit was 3–5°C higher than the ambient, because of the work done by the blower. The air jet attained ambient temperature, through diffusion of heat with the surrounding, at a nominal distance of approximately 120 mm. In order that the jet temperature at impingement was ambient for all sets of experiments, it was necessary to cool the compressed air before passing it through the nozzle, especially when the nozzle was located close (< 120 mm) to the heated plate. This was done by wrapping sections of the blower delivery pipe (uninsulated) with water cooled cotton-waste.

Power input to the heater assembly could be varied by means of an auto-transformer, resulting in different surface temperature for the plate. The measurements were carried out at steady state, which was generally after 3 hours of switching the power on, and measured by an invariance of temperature to within $\pm 0.1°$ over a 30 minute period. A sample measurement condition was 42 W input to the main heater, 18 W to the guard, plate to ambient temperature difference of 9.8°C, plate isothermality within ± 0.5°C, jet speed 32 m s^{-1}, nozzle distance 17 times the outlet diameter of 7 mm.

3.3. *Local heat flux*

The three-wire heat flux sensors [14, 15] located on the plate surface could simultaneously measure the local heat flux and plate temperature. The heat flux values, sensed through the differential thermocouple arrangement, was monitored by a Philips PM 2434 d.c. microvoltmeter with 0.1 μV resolution, whereas the temperature was measured by a Philips PP 9007 DMM. It will be recalled from ref. [14] that heat flux measurements using the differential sensor do not

need the value of the heat input. Heat losses from the module also do not influence the heat flux value read by a sensor.

As has been indicated earlier, and elaborated in refs. [14, 15], the calibrations of the sensors involved mounting three to four at a time on a thick-walled aluminium sphere, of 10 cm OD, with an internal heater fed from a controlled power supply. The heater is placed in a flow field of three pedestal fans to create uniform convection condition on its periphery. The heat flux on the sphere surface is then used to relate the differential thermocouple reading of each sensor.

The calibration constant varied for each of the sensors, and was between 90 to 175 μV $(\mathrm{W\ cm^{-2}})^{-1}$. A calibration is maintained if the foil thickness is not disturbed, and subsequent *in situ* measurements carried out under conditions of $Bi < 0.16$, where $Bi = hR^2/k_f t$ [14]. The above stipulations place a limit on the maximum value of the heat transfer coefficient that can be measured within the linear range of a sensor. Taking $R = 1$ mm, $t = 0.23$ mm and $k_f = 22$ $\mathrm{W\ m^{-1}\ K^{-1}}$ for the constantan foil, we get the limiting value as

$$h_{\max} \simeq 810\,\mathrm{W\ m^{-1}\ K^{-1}}. \quad (2)$$

3.4. *Uncertainty analysis*

From an analysis of the experimental uncertainty, it was found that the uncertainty in the determination of pressure (P_0) was about 0.1% and less than 0.16% for the jet temperature. The resulting uncertainty in the measured flow velocity was 1.25%. The overall uncertainty of the heat transfer coefficient (h) was estimated to be 2.14% at the lowest values of flow velocity. This decreased with increasing jet velocity.

4. RESULTS AND DISCUSSIONS

The impinging nozzle was positioned concentric with the heated plate, and was moved along the perpendicular axis of the plate to simulate different z/d ratios. The heat transfer coefficient at the location of a sensor was obtained from the value of the heat flux as well as the plate temperature read by the same sensor.

4.1. *Symmetry*

Confidence in the measured values, with each of the nozzles, was first ascertained from the readings of the sensors placed symmetrically around the plate centre. In Fig. 3, typical readings for the 5 mm nozzle are given for $Re = 24\,900$, $z/d = 58$ and $Re = 6860$ and $z/d = 15$. The symmetric nature of the Nusselt number values on either side of the centre-line is noted for both cases. The maximum deviation from symmetry was 7% for $z/d = 58$ down to 3% for $z/d = 15$. The Nusselt and Reynolds numbers are defined on the jet diameter and the jet velocity at the exit of the nozzle.

4.2. *Impingement point*

The peak heat transfer rate takes place at the location where the jet impinges on the plate. The highest value recorded at this point was nearly the same for all three cases: 765, 755 and 770 $\mathrm{W\ m^{-2}\ K^{-1}}$ for 3, 5 and 7 mm nozzles. Note that these values are less than the limiting one given in equation (2).

Sample variations of impingement point heat transfer are given in Fig. 4 for the three nozzles impinging from a fixed distance of $z = 75$ mm. The jet Reynolds number and the distance from the plate were varied over wide ranges for each of the three nozzles. It was observed that the peak heat transfer rate decreased faster with increasing nozzle distance when the nozzle outlet diameter was higher. The following correlations were arrived at by a regression analysis for each of the nozzles, within error limits mentioned alongside.

$d = 3$ mm

(i) $$Nu_0 = 0.150 Re^{0.701} (z/d)^{-0.250} \quad (3)$$

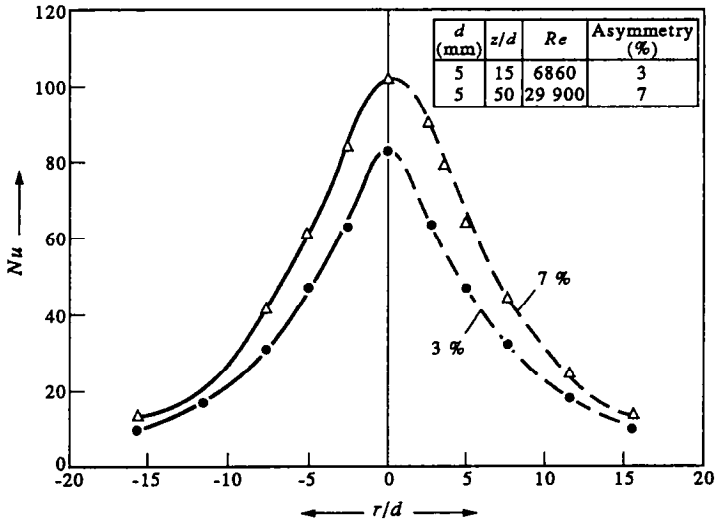

FIG. 3. Symmetry of sensor readings around the plate-centre.

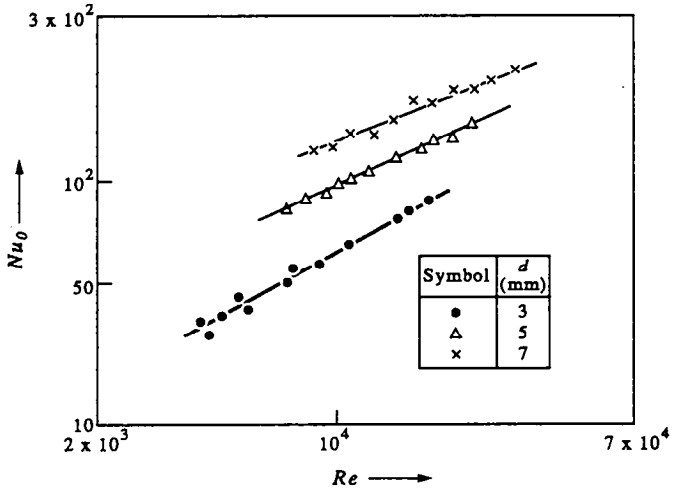

FIG. 4. Sample variations of impingement point heat transfer for $z = 75$ mm.

for $10 \leqslant z/d \leqslant 16.7$, standard deviation ($SD$) = 2%

(ii) $$Nu_0 = 0.170\, Re^{0.701}(z/d)^{-0.182} \quad (4)$$

$20 \leqslant z/d \leqslant 25$, $SD = 2.3\%$

both (i) and (ii) for $4860 \leqslant Re \leqslant 15\,300$.

$d = 5$ mm

$$Nu_0 = 0.388 Re^{0.696}(z/d)^{-0.345} \quad (5)$$

$6 \leqslant z/d \leqslant 58$, $6900 \leqslant Re \leqslant 24\,900$, $SD = 4.1\%$

$d = 7$ mm

$$Nu_0 = 0.615 Re^{0.670}(z/d)^{-0.380} \quad (6)$$

$9 \leqslant z/d \leqslant 41.4$, $7240 \leqslant Re \leqslant 34\,500$, $SD = 0.8\%$.

4.3. *Radial variations of h*

The three-wire heat flux sensors located along the quadrature axes, Fig. 2, about the impingement point yielded information on the radial variations of the heat transfer coefficient with changes in z/d and Re values. Sample results for the 5 mm nozzle at $Re = 17\,900$ are given in Fig. 5 when z/d was varied from 13.0 to 39.6. In Fig. 6, experimental results are presented for the 7 mm nozzle with $z/d = 9$ and Re varied from 8600 to 34 500.

Sparrow and Lovell [8] presented radial variations of Nu/Nu_0 for $z/d = 10$ and $Re = 5000$ using a 6.35 mm round nozzle and measurements by a naphthalene sublimation technique. In our experiments a low $Re = 4860$ could be simulated only with the 3 mm nozzle. Fixing the z/d at 10, we obtained a similar trend in the variations of Nu/Nu_0 as in ref. [8] and shown in Fig. 7. Quantitative deviation, small though it is, could be due to the difference in the diameters of the nozzles used in the two studies. We note for high Re at a given $z/d = 9$ in Fig. 6, that the heat transfer rate exhibits a local peak towards the plate edge. This phenomenon can be attributed to the tendency of the jet to reattach far from the point of impingement. Similar observations are made in Fig. 5, at $z/d = 13$ and a moderate $Re = 17\,900$.

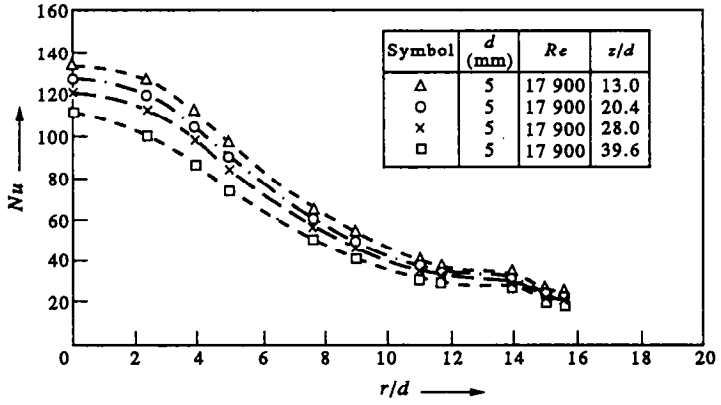

FIG. 5. Variation of Nusselt number for different z/d ratios, $Re = 17\,900$.

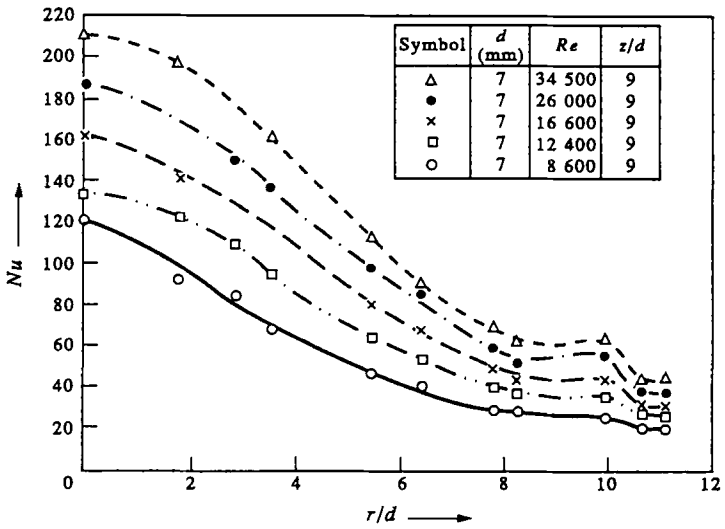

FIG. 6. Variation of Nusselt number at fixed z/d ratio and different Reynolds number.

Far away from the point of impingement, where the jet-effect is negligible, the heat loss from the plate is due to free convection. We denote this rate by h_f, and attempted a correlation for a heat transfer function

$$H = \frac{h - h_f}{h_0 - h_f} \tag{7}$$

h is the local value and h_0 is that at the stagnation point. If in practice there is a parallel flow, h_f may be assigned the value due to the parallel convection.

In arriving at the value of H, we used h_0 from equations (3)–(6) depending on the flow parameters, h measured at radius r and h_f from free convection correlations for horizontal heated circular plates, a recent summary of which is given in ref. [16]. The advantages of the definition for H, equation (7), are obvious. Its value is unity at the impingement point and is zero as $r \simeq \infty$.

From the measurements point of view, the impingement point is really of finite dimension; at the least it is equal to the size of the sensor (3 mm OD). When the nozzle is placed closed to the plate, however, the effective size of the impingement becomes larger, and we take it equal to the nozzle diameter.

The correlations given in each of the Figs. 8, 9 and 10 are made between $r = d/2$ to $r \simeq \infty$. The impingement point heat transfer rate h_0 is deemed to remain constant $r = 0$ to $d/2$. The correlations for the variation of local heat transfer are summarized here from Figs. 8, 9 and 10 in the manner

$$H = A\,e^{-m(r/d)} \tag{8}$$

where A and m are listed in Table 1.

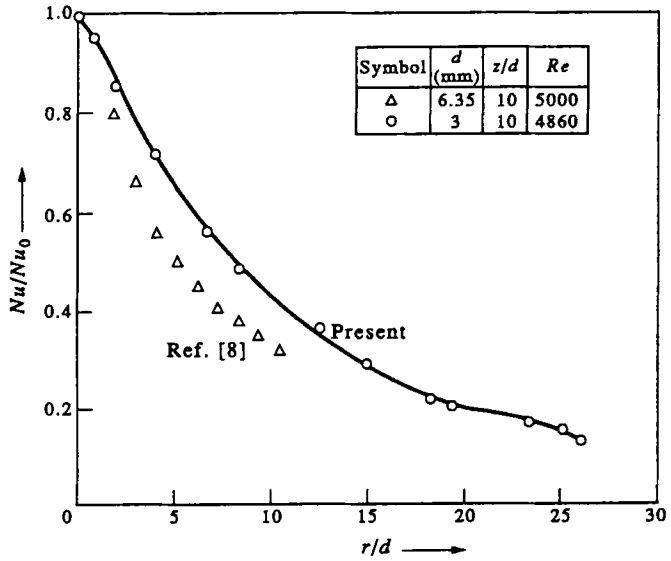

FIG. 7. Local heat transfer distribution.

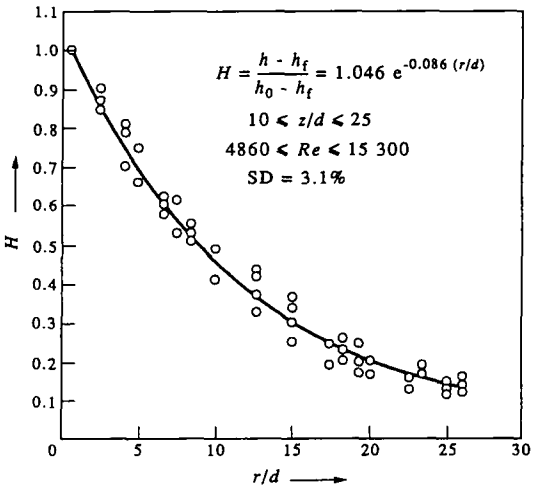

FIG. 8. Local heat transfer for a 3 mm nozzle.

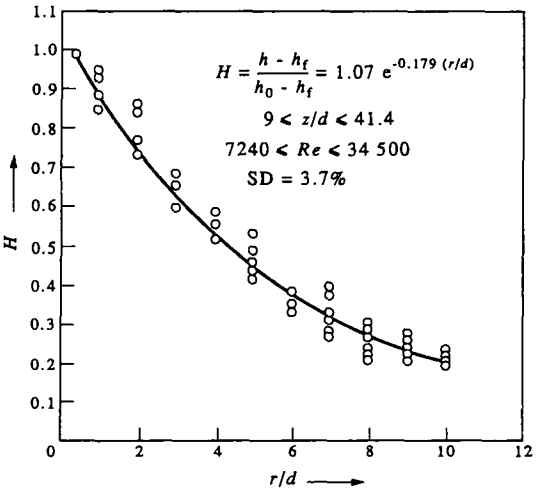

FIG. 10. Local heat transfer for a 7 mm nozzle.

Note that the correlation reproduces H at $r = d/2$ excellently for the 3 and 5 mm nozzles and with 2% deviation for the 7 mm nozzle.

4.4. *Effective radius*

We have indicated earlier that the effective cooling area due to an impinging jet has been chosen arbitrarily by different authors [6, 8]. We wish to propose a norm.

The exponential decay of H in equation (8) can be rewritten expressing the coefficient $A = e^n$, as

$$H = e^{-q} \tag{9}$$

where $q = n - m(r/d)$.

We define the effective radius for an impinging jet by setting $q = c$, the value of c being a designer's choice. For instance, with $c = 1$, the value of H is 0.368 at $r = r_{eff}$, with $c = 0.5$, H is 0.606, while with $c = 2$, H is 0.135.

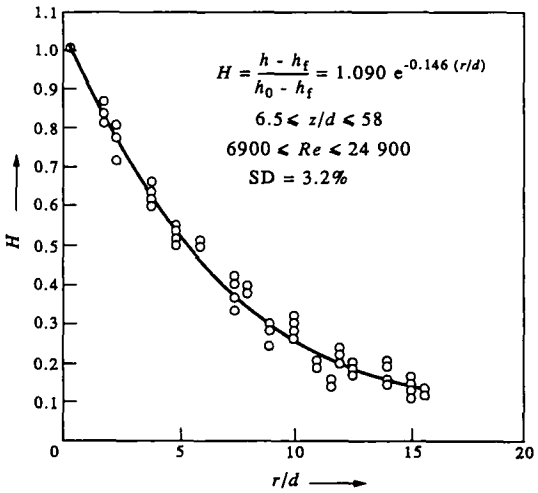

FIG. 9. Local heat transfer for a 5 mm nozzle.

We set $c = 1$ to define the effective radius and obtain

$$n - m(r/d) = -1$$

or

$$r_{eff} = \left(\frac{1+n}{m}\right) d. \tag{10}$$

The values of n and m are read from Table 1, yielding $r_{eff}/d = 12.15$, 7.34, 5.96 respectively for 3, 5 and 7 mm nozzles.

We observe that expression (10) for effective radius, derived with a physical criterion that $H_{r_{eff}} = e^{-1}$, covers the value of $r_{eff}/d = 4$–8 given by Sparrow and Lovell [8], and $r_{eff}/d = 12$ given by Huang [6]. These lend support to the choice of $c = 1$.

4.5. *Average heat transfer coefficient*

The identification of r_{eff} in equation (10) now affords a logical spatial limit for estimating the average heat transfer coefficient

$$\bar{H} = \frac{1}{\pi r_{eff}^2}\left[H_0 \frac{\pi d^2}{4} + \int_{d/2}^{r_{eff}} 2\pi r H\, dr\right] \tag{11}$$

$H_0 = 1$ corresponds to the uniform heat transfer rate between $r = 0$ to $d/2$ in Figs. 8, 9 and 10. In order to seek a convenient expression for $\bar{H}$ we extend the exponential curve to $r = 0$ and write equation (11) as

$$\bar{H} = \frac{1}{\pi r_{eff}^2} \int_0^{r_{eff}} 2\pi r H\, dr. \tag{12}$$

Table 1. Heat transfer correlation parameters

d (mm)	A	m	SD	H at $r/d = 0.5$	n
3	1.046	0.086	3.1%	1.001	0.0449
5	1.090	0.146	3.2%	1.010	0.0862
7	1.070	0.179	3.7%	0.978	0.0676

The error caused by this simplification is the near triangular area of the H–r curve, over the rectangular zone between $r = 0$ to $d/2$. The ratio of the area of the traingle to the rectangular for the uniform zone is $(A-1)/2H_0$, which has a maximum value of 0.045 for the 5 mm nozzle. Taken over the total area of the H–r curve, the error introduced is insignificant.

Substitution of $H = e^{n-m(r/d)}$ and integration yields

$$\bar{H} = \frac{2e^n}{r_{\text{eff}}^2}\left(\frac{d}{m}\right)^2[1-(2+n)e^{-(1+n)}] \qquad (13)$$

or

$$\bar{H} = \frac{2e^n}{(1+n)^2}[1-(2+n)e^{-(1+n)}] \qquad (14)$$

when expression (10) for r_{eff} is utilized.

Note that $\bar{H}$ is independent of the index m of the exponential decay of the jet-effect. Reading the values of n from Table 1, we get $\bar{H} = 0.5379$, 0.5467 and 0.5428 for the 3, 5 and 7 mm diameter nozzles. The value of $\bar{H} = 0.5284$ is attained for $n = 0$, i.e. $A = 1$. A comparison of the values, suggests a value of $\bar{H} = 0.54$ as a convenient design choice.

5. CONCLUSIONS

Local measurements of heat flux and temperature on a heated isothermal plate in the presence of an impinging jet quantified the dependence of the impingement point heat transfer coefficient h_0 on Reynolds number and the plate to nozzle distance. Beyond $d/2$, the heat transfer rate varies exponentially with the radial distance.

It is convenient to define an effective radius where the non-dimensional heat transfer rate H has decreased to e^{-1}. The definition $H = (h-h_f)/(h_0-h_f)$ duly accounts for the transport rates at impingement point and far away from that location. An average $\bar{H} = 0.54$, over the effective zone, applies well for all the three nozzles and flow rate conditions.

When multiple nozzles are intended to be used their pitch can be selected equal to $2r_{\text{eff}}$. The effective radius can be smaller or larger depending on the choice of the value of c, where $c = n-m(r/d)$, as warranted by the severity of heat removal condition. The heat transfer coefficient h_f can be utilized to model convections prevailing at the outer edge of the effective area. For example, h_f is assigned free convection value for a single nozzle, but should have the parallel flow transport rate value, if such a flow was present. h_f can be assigned the value due to a neighbouring nozzle, when the zones of influence of two closely spaced nozzles overlap such as in the case of $c < 1$.

REFERENCES

1. H. Martin, Heat and mass transfer between impinging gas jets and solids surface, *Advances in Heat Transfer* **13**, 1–66 (1977).
2. K. P. Perry, Heat transfer by convection from a hot gas jet to a plane surface, *Proc. of Inst. of Mech. Eng.* **158**, 775–780 (1954).
3. J. M. F. Vickers, Heat transfer coefficients between fluid jets and normal surfaces, *Industrial and Engineering Chemistry* **51**, 967–972 (1959).
4. R. Gardon and J. Cobonpune, Heat transfer between a flat plate and jets of air impinging on it, *Int. Development in Heat Transfer*, Proc. 2nd Int. H.T. Conf., ASME, NY, 1459–1460 (1962).
5. R. Gardon and J. C. Akfirat, Heat transfer characteristics of impinging two-dimensional air jet, *J. Heat Transfer* **88**, 597–606 (1966).
6. G. C. Huang, Investigations of heat transfer coefficients for air flow through round jets impinging normal to a heat transfer surface, *J. Heat Transfer* **85**, 237–245 (1963).
7. E. A. Vallies, M. A. Patrick and A. A. Wragg, Radial distribution of convective heat transfer coefficient between an axisymmetric turbulent jet and a flat plate held normal to the flow, *Proc. 6th Int. Heat Transfer Conference* **5**, 297–303 (1978).
8. E. M. Sparrow and B. J. Lovell, Heat transfer characteristics of an obliquely impinging circular jet, *J. Heat Transfer* **102**, 202–209 (1980).
9. N. T. Obot, A. S. Mujumdar and W. J. M. Douglas, The effect of nozzle geometry on impingement heat transfer under a round turbulent jet, ASME, 79-WA/HT-53 (1979).
10. S. X. Wang, Z. Dagan and M. L. Jili, Heat transfer between a circular free impinging jet and a solid surface with non-uniform wall temperature or wall heat flux—1. Solution for the stagnation point, *Int. J. Heat Mass Transfer* **32**, 1351–1360 (1989).
11. S. X. Wang, Z. Dagan and M. L. Jili, Heat transfer between a circular free impinging jet and a solid surface with non-uniform wall temperature or wall heat flux—2. Solution for the boundary layer region, *Int. J. Heat Mass Transfer* **32**, 1361–1371 (1989).
12. D. T. Vadet, F. P. Incropera and R. Viskanta, A method for measuring steady local heat transfer to an impinging liquid jet, *J. ETFS.* **4**, 1–11 (1991).
13. P. Hrycak, Heat transfer from round impinging jets to a flat plate, *Int. J. Heat Mass Transfer* **26**, 1857–1865 (1983).
14. B. V. S. S. S. Prasad and A. K. Mohanty, Analysis and calibration of foil heat flux sensor for convective measurements, *J. Phys. E: Sci. Instrum.* **16**, 1095–1099 (1983).
15. A. K. Mohanty and B. V. S. S. S. Prasad, Experimental study of heat transfer from pressure gradient surfaces, *J. ETFS.* **4**, 44–55 (1990).
16. M. Sahraoui, M. Kaviany and H. Marshall, Natural convection from horizontal disks and rings, *J. Heat Transfer* **112**, 110–116 (1990).